Volume 26
Number 3
7 February 2024
Pages 1025-1664

Green Chemistry

Cutting-edge research for a greener sustainable future

rsc.li/greenchem

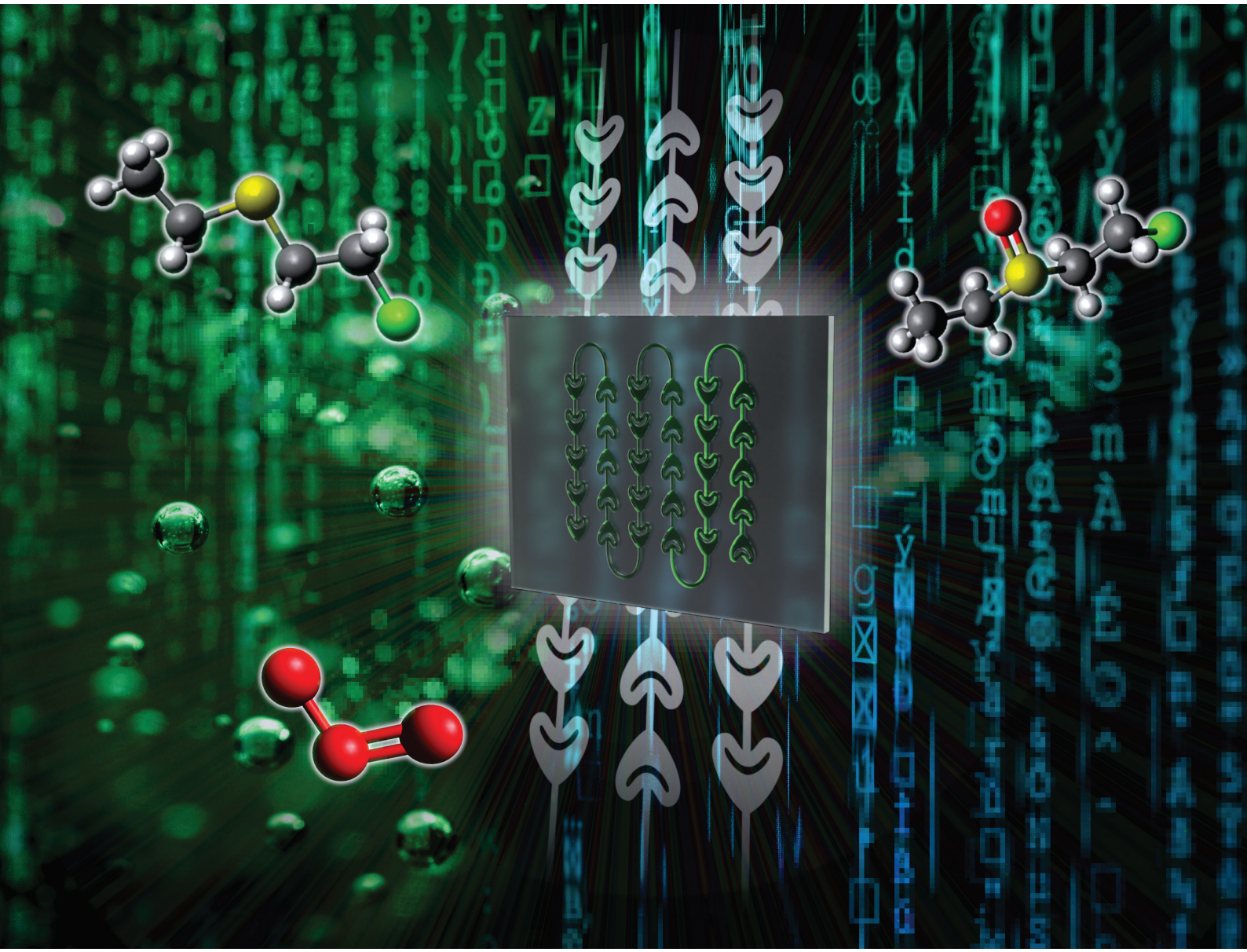

ISSN 1463-9262

ROYAL SOCIETY OF CHEMISTRY

COMMUNICATION

Julien Legros, Jean-Christophe M. Monbaliu *et al.*
A miniaturized ozonolysis flow platform for expeditious sulfur mustard warfare simulant neutralization

25 YEARS ANNIVERSARY

Green Chemistry

ROYAL SOCIETY OF CHEMISTRY

COMMUNICATION

View Article Online
View Journal | View Issue

Cite this: *Green Chem.*, 2024, **26**, 1281

Received 13th September 2023,
Accepted 16th October 2023

DOI: 10.1039/d3gc03470d

rsc.li/greenchem

A miniaturized ozonolysis flow platform for expeditious sulfur mustard warfare simulant neutralization†

Maxime Boddaert,‡[a,b] Pauline Bianchi,‡[a] Diana V. Silva-Brenes,[a,c] Ancuta Musina,[d] Marc Winter,[d] Philippe M. C. Roth,[d] Pierre-Yves Renard,[b] Julien Legros *[b] and Jean-Christophe M. Monbaliu *[a,c]

This communication introduces a highly efficient, safe and sustainable flow protocol for the oxidative neutralization of sulfur-based chemical warfare agent simulants using ozone. The methodology employs preliminary *in silico* mechanistic studies and chemical analogy studies with DFT to scout reaction profiles and kinetics. It unveils crucial parameters that guide selectivity and prevent the formation of undesirable overoxidized by-products. This computational foundation is seamlessly translated into real-world neutralization experiments conducted under flow conditions, yielding remarkably swift neutralization rates under mild conditions. Full oxidative neutralization of CWA simulants with ozone is achieved within a second, without the need for additives or catalysts, in an EtOH/water mixture. This convergence of computational insights and experimental validation provides a promising avenue toward new neutralization protocols, foreseeing transformative possibilities with low waste generation and high safety.

Introduction

Bis(2-chloroethyl)sulfide (aka sulfur mustard, mustard gas, yperite, or **HD**; CAS 505-60-2) was originally prepared by Guthrie and Niemann in 1860.[1,2] It was first weaponized during World War I as a vesicant, inducing severe skin and mucous membrane blistering upon contact. Its deployment on battlefields was prohibited with the Geneva Protocol (1925), and the manufacture, accumulation, and utilization of **HD** was again proscribed by the Chemical Weapons Convention (CWC) in 1997. The Organization for the Prohibition of Chemical Weapons (OPCW) and the CWC-signatory countries have relentlessly worked on the destruction of existing stockpiles.[3,4] These endeavors reached their culmination with a recent declaration from the US Department of Defense, confirming the successful destruction of domestic CWA stockpiles.[5]

With these significant achievements in disarmament, the interest for developing new neutralization protocols specifically targeting **HD** can be legitimately questioned. There are, however, other threatening scenarios involving **HD**. The countries that have not ratified the CWC, on the one hand, and the current geopolitical instabilities and terrorist threats on the other, are only the visible part of the iceberg. A silent, background threat of inestimable ecological and societal magnitude lies in the many maritime dump sites of CWAs remnants from World Wars I & II.[6,7] All of the aforementioned points provide ample reason for continued creative exploration aimed at enhancing the efficiency of neutralization, detection, and emergency protocols. Documentation of these research domains has been steadily growing.[8–13]

Protocols for the neutralization and/or destruction of **HD** are designed to impede the formation of an electrophilic episulfonium species, **epi-HD**, which is linked to the acute toxicity of sulfur mustards (Fig. 1a and b). The official method for destroying **HD** involves its direct incineration or the incineration of the corresponding hydrolysate after treatment under hot alkaline conditions.[14] Examples of solvolysis under hyperbaric conditions have also been reported,[15] as well as nucleophilic neutralization[16] and dehydrohalogenation protocols.[17] Selective sulfoxidation is by far the most reported protocol in the primary literature. It has been described through a multitude of variants including either (photo)catalytic or stoichiometric conditions (Fig. 1b).[10,11] Regardless of the conditions, the selectivity of the oxidation is the most critical parameter often at the expense of the atom economy, production costs, toxicity and practical considerations. Overoxidation to the

[a]*Center for Integrated Technology and Organic Synthesis, MolSys Research Unit, University of Liège, B-4000 Liège (Sart Tilman), Belgium.*
E-mail: jc.monbaliu@uliege.be; https://www.citos.uliege.be
[b]*Univ Rouen Normandie, INSA Rouen Normandie, CNRS, Normandie Univ, COBRA UMR 6014, INC3M FR 3038, F-76000 Rouen, France*
[c]*FloW4all Flow Technology Resource Center, University of Liège, B-4000 Liège (Sart-Tilman), Belgium*
[d]*Corning Reactor Technologies, Corning SAS, 7 bis, Avenue de Valvins CS 70156 Samois sur Seine, 77215 Avon Cedex, France*

†Electronic supplementary information (ESI) available: Fluidic components, computational protocols, experimental procedures, details of the fluidic setup and procedures, computational details, details for the off-line analyses (GC, HPLC) and structural assignments (NMR). See DOI: https://doi.org/10.1039/d3gc03470d

‡These authors contributed equally to this work.

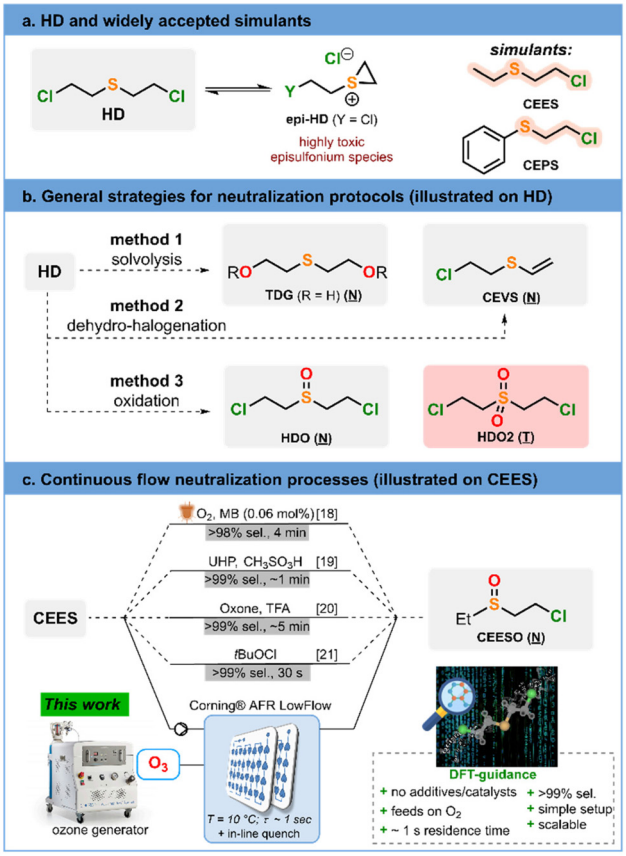

Fig. 1 Protocols for the chemical neutralization of **HD** and simulants. (**N**) refers to neutralized, low toxicity species, while (**T**) refers to toxic byproducts. (a) Structure of **HD**, its toxic episulfonium derivative (**epi-HD**), and widely accepted lower toxicity simulants (**CEES** and **CEPS**). (b) General protocols for the neutralization of **HD** and simulants, including solvolysis, dehydrochlorination and oxidation. (c) Continuous flow oxidative neutralization processes using either (photo)catalytic or stoichiometric conditions. The main strategy presented in this communication is illustrated.

corresponding toxic sulfone must be rigorously prevented. Indeed, the corresponding overoxidized sulfone, **HDO_2** (Fig. 1b), spontaneously forms a toxic divinyl sulfone through dehalogenation under physiological conditions. The latter has been associated with stronger protein denaturing properties than the parent **HD**.[18]

In a series of previous articles, we have documented our efforts to develop efficient oxidative neutralization flow processes specifically targeting **HD** simulants (*e.g.*, **CEES** or **CEPS**).[19–22] We believe that such protocols must rely on simple, widely available chemicals (Fig. 1c) in order to facilitate their widespread adoption in emergency situations. Our efforts also aim for low toxicity and safe process conditions. In addition, we have introduced innovation through the use of advanced computational methods, to both guide and further validate the neutralization processes on actual CWAs *in silico*.[19,22] Such a multidisciplinary approach offers safer and more sustainable options to address this challenging research area, with limited waste generation and chemical hazards for the operators. Despite these innovations, we sought to further improve the overall neutralization efficiency with extremely short reaction times and additive-, catalyst-free procedures to ease their implementation for emergency situations.

In this communication, we present a highly effective and sustainable protocol for the oxidative neutralization of **HD** simulants utilizing ozone under continuous flow conditions. The generation of ozone directly from compressed oxygen obviates the need for supplementary additives or catalysts, thereby fully harnessing its inherent oxidative potential. Our initial exploration encompassed *in silico* analyses using a DFT protocol, to elucidate the mechanism, selectivity, and intrinsic features. Additionally, we illustrate a rational selection process for low toxicity simulants of **HD** employing conceptual DFT to identify thioethers with analogous chemical behavior while mitigating the legal and toxicity concerns associated with **HD**. Computational profiles and kinetics of reactions *in silico* were computed to emphasize the most influential parameters driving selectivity and preventing the formation of toxic overoxidized by-products (sulfone derivatives). The computational work was next translated to actual neutralization experiments conducted under flow conditions, yielding unprecedently fast neutralization rates (full neutralization within a mere second). We believe that this multidisciplinary approach surpasses existing protocols that rely exclusively on experimental data or on cheminformatics protocols.[23]

Experimental section

General information

Samples were analyzed by gas chromatography coupled to flame ionization detection (GC-FID, Shimadzu GC-2014) or by high performance liquid chromatography coupled to diode-array detection (HPLC-DAD, Shimadzu Prominence LC-2030 3D). Structural identity was confirmed by ^{1}H and ^{13}C NMR spectroscopy (400 MHz Bruker Avance spectrometer), and by GC-MS (ESI, section 6†). Methyl phenyl sulfide (**1a**), methyl phenyl sulfone (**3a**), dipropyl sulfide (**1b**), dipropyl sulfone (**3b**), 2-chloroethyl phenyl sulfide (**CEPS**), 2-chloroethyl phenyl sulfone (**$CEPSO_2$**), 2-chloroethyl ethyl sulfide (**CEES**), 2-chloroethyl ethyl sulfone (**$CEESO_2$**), ethanol, water, and sodium thiosulfate were purchased from commercial sources and used without additional purification (ESI, section 3.1†). Methyl phenyl sulfoxide (**2a**), dipropyl sulfoxide (**2b**), 2-chloroethyl phenyl sulfoxide (**CEPSO**), and 2-chloroethyl ethyl sulfoxide (**CEESO**) were prepared according to protocols from the literature.[24,25]

Computational study

Calculations were performed using the Gaussian 16 [26] package and implicit solvation (SMD, solvent = ethanol). Optimization and characterization with vibrational analysis of the stationary points were carried out at the B3LYP-D3BJ/6-31+G* level of

theory. Electronic energies were computed at the M08HX/6-311+G** level whereas solvation energies and Gibbs free energy corrections were obtained at the B3LYP-D3BJ/6-31+G* level. Transition states (TSs) were determined with the Newton–Raphson technique, then checked with the Hessian matrix and intrinsic reaction coordinates (IRC). The lowest energy conformation for each transition state was kept when determining activation barriers. Activation barriers were corrected for concentration and quasi-harmonic factors (Grimme method for entropy and Head-Gordon method for enthalpy correction)[27] using our open-access SnapPy toolkit (v1.0.0.).[28] Reaction times were also determined using SnapPy. NBO charges were calculated using the NBO 3.1 extension from Gaussian. Local nucleophilicity on the sulfur atom was calculated using equations from conceptual density functional theory.[29,30] All equations and the protocols followed are available in the ESI (section 1.1†).

Safety statement

CAUTION: 2-Chloroethyl phenyl sulfide (**CEPS**) and 1-chloro-2-(ethylsulfinyl)ethane (**CEES**) are highly toxic and severe vesicants and must be handled under a fume hood. All contaminated glassware should be neutralized with bleach prior to disposal (be warned that the quench solution containing sodium thiosulfate is chemically not compatible with bleach). Ozone is toxic and a strong oxidizer. All experiments should be carried out under a fume hood in the presence of a fully qualified ozone detector. For additional safety, it is recommended that the operator possesses a portable personal ozone detector at all times during operations. Ozone can also form peroxides with various organic compounds; therefore, it is recommended to regularly use peroxide test strips on reactor effluents before disposal. Ozone decomposes resulting in the formation of oxygen and therefore potentially forming a flammable oxygen/solvent mixture. To mitigate this risk, it is strongly recommended to degas and dilute the reactor effluent with a continuous stream of nitrogen. Additional details on the safety measures are detailed in the ESI (section 4†). The readers should become aware of legal restrictions in their country on the permittance to study **HD** or any related analogs of chemical warfare agents before possessing them in the lab.

Optimized conditions for the oxidative neutralization of CEES (0.5 M)

Lab scale mesofluidic experiments were carried out in a Corning® Advanced-Flow™ LowFlow reactor (0.5 mL internal volume glass fluidic modules) connected to a Corning Ozone generator. Liquid feeds were handled with syringe or piston pumps (Knauer – Azura P4.1S for the feed solution A containing the sulfide; HiTec Zang SyrDos™ 2 XLP for feed B containing the quench solution). Feed and collection lines consisted of PFA tubing (1/8″ o.d.) with PFA or stainless steel (SS) Swagelok connectors and ferrules. The process temperature was regulated with a LAUDA PROLINE RP 845 thermostat. The downstream pressure was set at 10 bar (Zaiput BPR-10). The reactor setup was thoroughly flushed with nitrogen, and then with 1 : 1 EtOH/H_2O mixture for 5 min. The pump handling feed solution B (0.5 M sodium thiosulfate quench solution in 9 : 1 (v : v) water/ethanol mixture) was set to 3.51 mL min^{-1} and the pump handling feed solution A (0.5 M **CEES** in EtOH) was set to 1.76 mL min^{-1}. Lastly, the line feeding the reactor with ozone (282 mL_N min^{-1}) was initiated. **CEES** was reacted with ozone at 10 °C for a residence time of 1 s. Samples were collected at steady state. Note that the selection of a 9 : 1 (v : v) water/ethanol mixture is critical to avoid extensive precipitation of inorganic salts upon quenching. After each run, the ozone gas line was redirected to the vent, and the generator and lines were flushed with nitrogen.

Results and discussion

Computational design

The access to **HD** is restricted to very few labs worldwide with military clearance. While such restriction is perfectly understandable given all the above, it is clearly a main limitation when it comes to the development of actual **HD** neutralization protocols. Safety concerns are enough to trigger the search for alternative, low-toxicity structures, yet able to provide relevant chemical information. There is a wide range of commercially available thioethers, and among them, both **CEPS** and **CEES** are commonly used **HD** simulants due to their structural resemblance. However, both compounds are toxic and severe vesicants, and their use should not be taken lightly for the development of neutralization processes. Other suitable commercially available thioethers may exist, however sufficient quantitative information is necessary to support their use as potential simulants. In an ideal scenario, a low toxicity, widely available thioether would be used to develop new process conditions, prior to transposition to a closer **HD** simulant. A quantitative metric to claim chemical analogy between such a thioether and **HD** can be accessed *in silico*. The availability of the non-bonding n_S orbitals through stereoelectronic interactions has been already proposed by our lab as a first metric to rank the potential candidates,[19] though it was based only on chemical intuition. We have now developed the necessary tools and know-how for accessing a more refined selection protocol. The latter relies both on conceptual density functional theory (CDFT)[29,30] and on the accurate calculation of activation barriers through our open-source software.[28] The combination of both provided a powerful tool to extract the information necessary to draw chemical analogies between the species. We believe that the increasing reliance on *in silico* methods to predict chemical behavior can also contribute to reducing the amount of waste generated in experimental trial-and-error and optimization phases, specifically when toxic compounds are involved.[31]

In the presence of ozone, the sulfur atom of **HD** is expected to behave as a nucleophile,[32] which is confirmed by the computations of the reaction mechanism (see below). Therefore, the local nucleophilicity (N_S)[29] on the sulfur atom of **HD** and six potential simulants was computed at the

B3LYP-D3BJ/6-31+G* level in ethanol (Fig. 2a) using a classical approach in CDFT. The six potential thioether simulant candidates included methyl phenyl sulfide (**1a**), dipropyl sulfide (**1b**), diphenyl sulfide (**1c**), dibenzo[*b*,*d*]thiophene (**1d**), 2-chloroethyl phenyl sulfide (**CEPS**) and 2-chloroethyl ethyl sulfide (**CEES**).

The local nucleophilicity on **1b** (N_S = 2.1) emphasizes a stronger nucleophilic behavior than the other computed thioethers. Conversely, **1c** (N_S = 1.0) and **1d** (N_S = 0.8) appeared at the antipode, their nucleophilicity being reduced through delocalization. **CEES** (N_S = 1.9), **1a** (N_S = 1.8) and **CEPS** (N_S = 1.6) demonstrated local nucleophilicities akin to **HD** (N_S = 1.8). This initial analysis underscores **1a** and **CEES** as the closest **HD** simulants in terms of local nucleophilicity. Refining the analysis through the computation of molecular electrostatic potential (MEP) surfaces corroborated the CDFT trends. MEP surfaces also reveal the intense electron-withdrawing effect of chlorinated substituents (Fig. 2a), thus providing more insight into the necessary requirements to mimic the reactivity of **HD**. From there, it became apparent that **1a** is a promising simulant for **HD**, given its low toxicity compared to **CEES**. While being structurally different, it mimics the nucleophilicity of the sulfur atom on **HD**, yet it lacks the activated C–Cl bond. **CEES** is the most trustworthy simulant, combining both similar sulfur local nucleophilicity and the influence of at least one activated C–Cl bond. On the other hand, despite structural proximity to **CEES**, **CEPS** does not emerge as an optimal simulant, with a decreased N_S, which likely entails distinct chemical behavior.

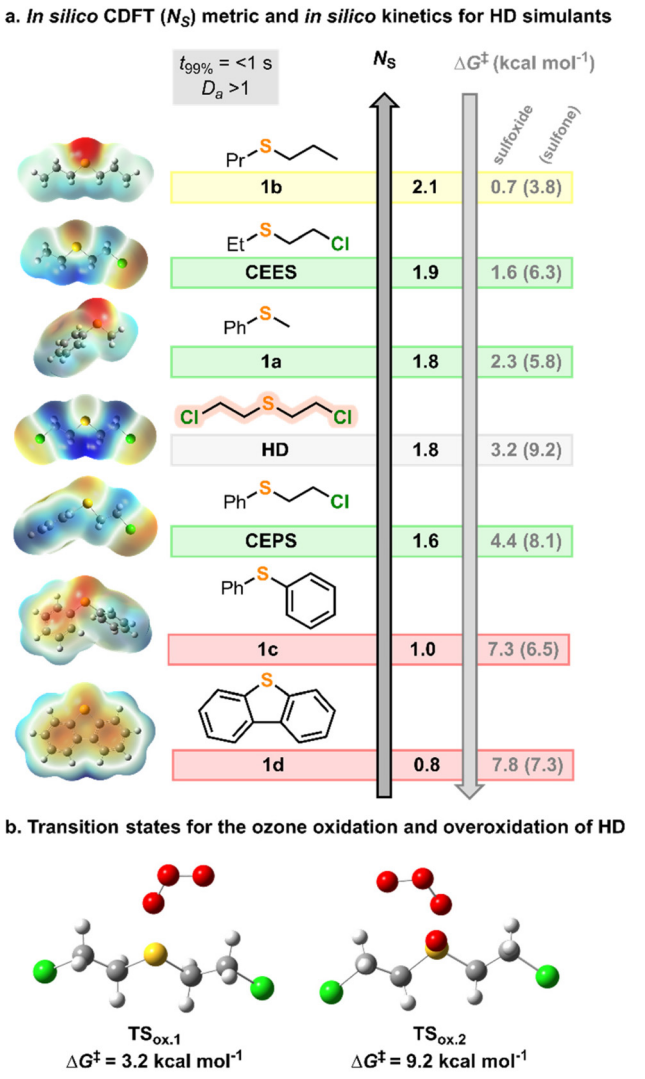

Fig. 2 (a) *In silico* **HD** simulant selection at the B3LYP/6-31+G*//M08HX/6-311+G** level (SMD = EtOH) (ESI, section 1.2†). N_S refers to the local nucleophilicity at the sulfur atom; $\Delta G^{\ddagger}$ is the activation barrier for the sulfoxidation, and for the overoxidation to sulfone (in brackets); $t_{99\%}$ is the time to reach 99% conv. of the substrate at 0.1 M and 10 °C; D_a is the Damköhler number. Inserts on the left-hand side depict the molecular electrostatic potential (MEP) surfaces (in red: negative potential up to −0.03 au, in blue: positive potential up to 0.03 au). Color code: green, good simulants for **HD**; yellow, average simulants for **HD**; red, poor simulants. (b) Transition state structures (B3LYP/6-31+G*) and activation energies for the oxidation of **HD** toward **HDO** and $\mathbf{HDO_2}$ (ESI, sections 1.3 and 1.4†).

The relevance of the sulfur local nucleophilicity as a suitable metric for the selection of **HD** simulants was further validated *in silico*. Transition states associated with the oxidation of thioethers **1a–d**, **CEPS**, **CEES** and **HD** were computed in EtOH toward the corresponding sulfoxides **2a–d**, **CEPSO**, **CEESO** and **HDO**, as well as for the undesired overoxidation to sulfones **3a–d**, $\mathbf{CEPSO_2}$, $\mathbf{CEESO_2}$ and $\mathbf{HDO_2}$ (Fig. 2a, b and ESI, sections 1.3 and 1.4†). The corresponding activation barriers ($\Delta G^{\ddagger}$) follow a similar trend to the local nucleophilicity index, as illustrated in Fig. 2a. In general, the higher the sulfur local nucleophilicity, the lower the activation barrier, at least for the critical sulfoxidation. These activation barriers can be connected to inherent kinetics through Eyring's equation (ESI, section 1.1†). For the sulfoxidation, the oxidations of all thioether substrates are characterized by low activation barriers ($\Delta G^{\ddagger}$ < 8 kcal mol^{-1}), which translates to reaction completion below 1 s (at 10 °C and 0.1 M). The overoxidation to the undesired sulfones comes with a higher activation barrier, at least for substrates **1a,b**, **CEPS**, **CEES** and **HD** (3.1 < $\Delta\Delta G^{\ddagger}$ < 6 kcal mol^{-1}). For compounds **1c,d**, the overoxidation appears to be more favorable than the sulfoxidation by 0.5–0.8 kcal mol^{-1}. Nevertheless, computational results confirm selectivity issues in all instances, since the activation barriers for overoxidation also translate into extremely fast kinetics, with 99% conversion expected below 1 s under the same conditions. It can therefore be concluded that these reactions are clearly limited by diffusion (D_a > 1)[33] and require high mixing efficiency to avoid concentration gradients. Selectivity towards the sulfoxide will therefore critically depend on both the selection of an appropriate setup allowing for short reaction times and high mixing efficiency, as well as an appropriate quenching of any remaining ozone.

This scenario emphasizes a case where conventional batch protocols encounter challenges in fulfilling these criteria. Furthermore, batch ozonolysis typically demands sub-zero temperatures to mitigate the potential for explosive reactions.

This prompted us to develop flow conditions, where dedicated flow reactors are meticulously engineered to sustain optimal mixing efficiency. Both the ability to integrate *in situ* quenching capabilities and the absence of headspace were also considered as important safety features for potentially flammable and/or explosive mixtures.[34]

Experimental validation

There is precedent for the ozonolysis of various substrates under continuous flow (micro and mesofluidic setups).[35–41] Here, experiments were performed using a commercial Corning® Advanced-Flow™ reactor (AFR) specifically designed for a minimal footprint (AFR™ LowFlow). The reactor configuration featured 2 LowFlow glass fluidic modules (FM, 0.5 mL internal volume each) specifically designed for high mass transfer in liquid–gas biphasic systems. Both FMs were connected in series and featured an embedded high-performance heat exchanger. The reactor setup was fed upstream with compressed ozone (10 bar) and with a liquid feed of thioether in ethanol. The pressurized ozone generator has been reported elsewhere.[35] FM1 was used for the oxidation of various **HD** thioether simulants with ozone, while FM2 was used to quench the reaction mixture (aqueous sodium thiosulfate, 0.5 M). Note here that the in-line quench is an additional safety feature to neutralize any unreacted ozone prior to the collection of reaction effluents. The reactor effluents were analyzed either by HPLC or GC-FID (ESI, section 3.2†). A simplified flow chart for the ozone neutralization platform is depicted in Fig. 3a (ESI, section 2 and 4† for detailed setup and experimental protocols, photos, and risk analysis).

Validation of the *in silico* predictions was next performed. Among the small libraries of potential **HD** simulants, 3 thioethers were picked to experimentally represent 3 different computed local nucleophilicities. Specifically, we chose to explore **1a** (N_S 1.8), as the most similar analogue to **CEES** (N_S 1.9) according to our computations; **1b** (N_S 2.1) as an example of a sulfide with a higher nucleophilicity than **CEES**; and **CEPS** (N_S 1.6) as an analogue with lesser reactivity and that is frequently used as a **HD** simulant. The conditions selected for the computational kinetics study were implemented experimentally, *i.e.*, 0.1 M concentration of the sulfide in EtOH and 1 s of residence time. A control experiment where the system was operated without ozone led to no conversion of the sulfide (Table 1, entry 1). Each of the selected compound was then tested using a small excess of ozone (1.4 equiv.) in order to test their propensity for overoxidation to the corresponding sulfones (**3a,b** and **CEPSO$_2$**). Under these conditions, the reaction with **1a** led to full conversion into its corresponding sulfoxide **2a**, with no overoxidation to sulfone **3a** (Fig. 3 and Table 1, entry 2). Sulfide **1b**, on the other hand, was converted into a mixture of the desired sulfoxide **2b** (96%) and sulfone **3b** (4%) (Fig. 3 and Table 1, entry 3). The overoxidation is not surprising considering the preliminary computational study, which revealed the higher nucleophilicity of **1b**. Finally, in the case of **CEPS**, the oxidation did not complete within the 1 s timeframe (Fig. 3 and Table 1, entry 4), affording only 81% of

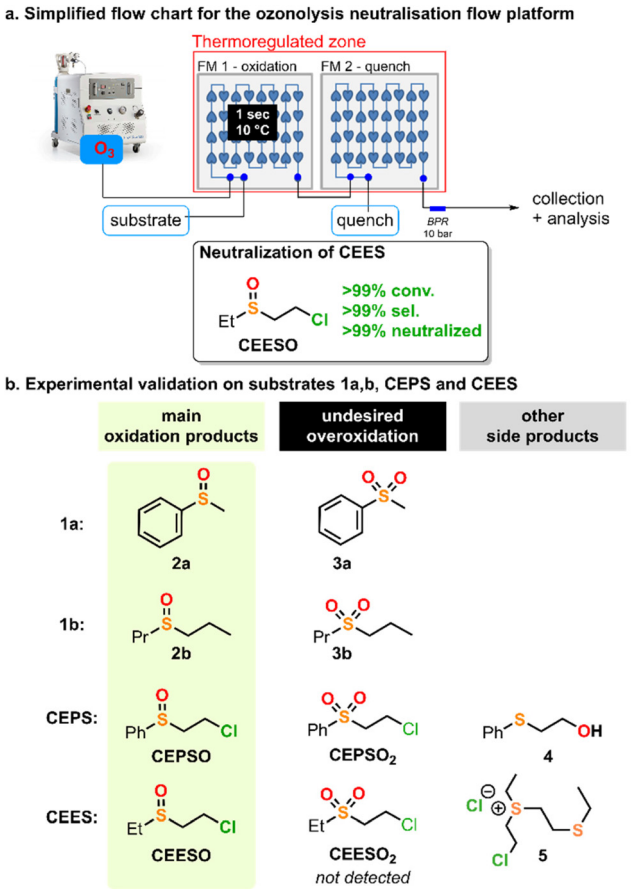

Fig. 3 (a) Simplified flow chart. (b) Structure of the different products observed upon ozone oxidation of compounds **1a,b**, **CEPS**, and **CEES** in the crude reactor effluents (see Table 1). Feed solutions for compounds **1a,b**, **CEPS**, and **CEES** were prepared in EtOH (0.1 or 0.5 M, see Table 1). The reactor effluent was quenched with 0.5 M aqueous sodium thiosulfate. All experiments were monitored with an ozone detector at the outlet of the reactor.

Table 1 Oxidative neutralization with ozone under flow conditions (see Fig. 3)

Entry	Substrate[a]	Ozone (equiv.)	Sulfide (%area)	Sulfoxide (%area)	Other products (%area)
1	**1a**	—	>99	n.d.	n.d.
2	**1a**	1.4	n.d.	>99	n.d.
3	**1b**	1.4	n.d.	96	**3b** (4)
4	**CEPS** [b]	1.4	9	81	**CEPSO$_2$** (2) **4** (8)
5	**CEES**	1.2	n.d.	>99	n.d
6	**CEES**	1	n.d.	>99	n.d.
7	**CEES**	0.8	>99	84	**5** (16)
8	**CEES** [c]	1	n.d.	>99	n.d.

[a] All experiments were carried out at 0.1 M and 10 °C with a backpressure of 10 bar. All samples were quenched with aqueous sodium thiosulfate (0.5 M). Data from LC (**1a**, **CEPS**) or GC-FID (**1b**, **CEES**) analysis (n.d. stands for not detected). [b] 0.2 M. [c] 0.5 M.

the sulfoxide **CEPSO** and 2% of the sulfone **CEPSO$_2$**. Part of the un-oxidized **CEPS** was hydrolyzed under the quench conditions, leading to the formation of compound **4** (8%). All these results agree with the *in silico* ranking and confirmed the sulfide nucleophilicity as a robust metric for the propensity of oxidation using ozone. Considering that **1a** is the closest analogue to **CEES** and having shown that **1a** could be fully and selectively oxidized to the sulfoxide using this method, we proceeded to test the protocol to neutralize **CEES**.

The neutralization of **CEES** using 1.2 equivalents of ozone successfully afforded full oxidation to the sulfoxide, while avoiding the formation of toxic sulfone **CEESO$_2$** (Table 1, entry 5). Trials using 1 equiv. of ozone showed equally satisfactory results, promoting full conversion towards sulfoxide **CEESO** (Table 1, entry 6). When substoichiometric amounts of ozone (0.8 equiv.) were used, only 84% of **CEES** was oxidized to **CEESO** (Table 1, entry 7). The remaining **CEES** reacted to form compound **5** (16%). The formation of compound **5** likely takes place during the quenching, through the formation of the episulfonium followed by nucleophilic attack from a second molecule of **CEES**. The presence of different side products for unreacted **CEES** or **CEPS** under the quenching conditions highlights the difference in nucleophilicity between both species. In water, mustard species are known to favor the electrophilic episulfonium form, which is then prone to react with nucleophilic species. While the sulfur atom of **CEES** is reactive enough to give product **5**, water competes with **CEPS** and forms hydrosylate **4**.[42]

Finally, to show the potential for higher throughput, the concentration of the feed solution of **CEES** was increased (0.5 M in EtOH). Using the same protocol, complete and selective conversion to the sulfoxide was obtained within 1 s (Table 1, entry 8).

Conclusion

We have developed an innovative protocol for the oxidative neutralization of **HD** simulants with unprecedented efficiency (0.5 M and 1 s residence time). This procedure harnesses the benefits of continuous flow to maximize the potent oxidizing nature of ozone. The methodology incorporates an initial DFT study to rationally guide the selection of appropriate simulants for **HD** oxidative neutralization processes and collect critical information on kinetics and selectivity, while preventing the generation of unnecessary waste. We demonstrate the relevance of the local nucleophilicity of sulfur as a metric for ranking simulants. This valuable approach could also be extended for studying non-toxic mustard analogues such as carbonates, which have already found synthetic applications in green chemistry.[43,44] As far as oxidative pathways are concerned, methyl phenyl sulfide (**1a**) appears as a good, low toxicity simulant for preliminary scouting of reaction conditions. Between two of the most widely used simulants, namely, 2-chloroethyl phenyl sulfide (**CEPS**) and 2-chloroethyl ethyl sulfide (**CEES**), CDFT descriptors emphasize **CEES** as the best choice. We have also demonstrated how *in silico* kinetics can be generated to frame experimental conditions and to highlight the critical parameters to be taken into consideration for efficient and selective processes. The sulfoxidation of selected thioethers proceeds with extremely fast kinetics primarily limited by diffusion. Subsequently, we successfully transitioned to a compact and efficient flow setup that guarantees optimal mixing, short residence times, in-line quench and superior selectivity. After experimental validation of the computational study, the most promising simulant **CEES** could be fully converted to the non-toxic sulfoxide species (>99% selectivity). The protocol herein described appears as one of the safest, most sustainable and compact oxidative neutralization processes: it uses mild conditions (10 °C, 10 bar of counterpressure), relies on EtOH/water as a solvent, and requires neither an additive nor a catalyst. This approach can be seamlessly integrated with widely accessible industrial ozone generators. This process is amenable to much larger scales based on the unique features of Corning AFR mesofluidic systems, ensuring seamless scalability to up to several liters per minute of processed material with larger mesofluidic reactors.[19,45–48] Finally, we would like to highlight the convergence between computations and experiments as a promising tool for accessing meticulously designed protocols and substantially reducing contact with highly toxic compounds such as **CEES**. These findings hold substantial promise for their extension to the neutralization of sulfur mustard **HD**.

Author contributions

MB performed the experiments. PB designed and performed the computational study, analyzed the results, and prepared the corresponding section in the manuscript and ESI.† DVSB supervised the experiments, wrote the experimental sections of the ESI,† and proofread the manuscript. AM, MW and PMCR commissioned the mesofluidic reactor setup and the ozone generator, provided technical assistance for the experimental optimization, and proofread the manuscript. JL and PYR designed the experiments and corrected the manuscript. JCMM designed the experiments, supervised the research, and wrote the manuscript.

Conflicts of interest

There are no conflicts to declare.

Acknowledgements

Computational resources were provided by the "Consortium des Équipements de Calcul Intensif" (CÉCI), funded by the "Fonds de la Recherche Scientifique de Belgique" (F.R.S.-FNRS) under grant no. 2.5020.11a and by the Walloon Region. PB is a F.R.S.-FNRS PhD fellow (ASP PhD fellowship 1. A.054.21F). This work was supported by the University of

Liège, the F.R.S.-FNRS (incentive grant for scientific research MIS F453020F, JCMM), and Corning SAS. The authors also thank Labex SynOrg (ANR-11-LABX-0029), Carnot Institute I2C, the graduate school for research XL-Chem (ANR-18-EURE-0020 XL CHEM) and the Région Normandie. The authors acknowledge Audrey Courboin (Corning SAS) for her technical support.

References

1 F. Guthrie, *Q. J., Chem. Soc., London*, 1860, **12**, 109–126.
2 A. Niemann, *Justus Liebigs Ann. Chem.*, 1860, **113**, 288–292.
3 UNODA, Chemical Weapons, **https://disarmament.unoda.org/wmd/chemical/**, (accessed 20 August 2023).
4 OPCW, What is a Chemical Weapon?, **https://www.opcw.org/our-work/what-chemical-weapon**, (accessed 20 August 2023).
5 United States Government, US Completes Chemical Weapons Stockpile Destruction Operations, **https://www.defense.gov/News/Releases/Release/Article/3451920/us-completes-chemical-weapons-stockpile-destruction-operations/**, (accessed 20 August 2023).
6 I. Wilkinson, Chemical Weapon Munitions Dumped at Sea: An Interactive Map | James Martin Center for Nonproliferation Studies, **https://nonproliferation.org/chemical-weapon-munitions-dumped-at-sea/**, (accessed 20 August 2023).
7 H. Sanderson, P. Fauser, M. Thomsen, P. Vanninen, M. Soderstrom, Y. Savin, I. Khalikov, A. Hirvonen, S. Niiranen, T. Missiaen, A. Gress, P. Borodin, N. Medvedeva, Y. Polyak, V. Paka, V. Zhurbas and P. Feller, *Environ. Sci. Technol.*, 2010, **44**, 4389–4394.
8 P. Kalita, R. Paul, A. Boruah, D. Q. Dao, A. Bhaumik and J. Mondal, *Green Chem.*, 2023, **25**, 5789–5812.
9 C. R. Jabbour, L. A. Parker, E. M. Hutter and B. M. Weckhuysen, *Nat. Rev. Chem.*, 2021, **5**, 370–387.
10 E. Oheix, E. Gravel and E. Doris, *Chem. – Eur. J.*, 2021, **27**, 54–68.
11 B. Picard, I. Chataigner, J. Maddaluno and J. Legros, *Org. Biomol. Chem.*, 2019, **17**, 6528–6537.
12 P. Kalita, R. Paul, C. W. Pao, R. Chatterjee, A. Bhaumik and J. Mondal, *Chem. Commun.*, 2023, **59**, 5067–5070.
13 M. Yu, J. Liu, F. Liu, F. Zou, L. Zhang, Q. Gao, X.-Y. Ren, Q. Zhang, S.-Z. Liu, C.-P. Dong, T.-T. Guo, T.-F. Ma and W.-Y. Pei, *Eur. J. Inorg. Chem.*, 2023, **26**, e202300221.
14 A. C. W. Alternatives, Program Executive Office, **https://www.peoacwa.army.mil/**, (accessed 20 August 2023).
15 S. Mansour, V. B. Silva, E. S. Orth and J. Legros, *Org. Biomol. Chem.*, 2022, **20**, 7604–7608.
16 V. B. Silva, S. Mansour, A. Delaune, F.-X. Felpin and J. Legros, *React. Chem. Eng.*, 2023, **8**, 2658–2663.
17 G. W. Wagner, P. W. Bartram, O. Koper and K. J. Klabunde, *J. Phys. Chem. B*, 1999, **103**, 3225–3228.
18 J. C. Boursnell, G. E. Francis and A. Wormall, *Biochem. J.*, 1946, **40**, 737–742.
19 N. Emmanuel, P. Bianchi, J. Legros and J.-C. M. Monbaliu, *Green Chem.*, 2020, **22**, 4105–4115.
20 B. Picard, B. Gouilleux, T. Lebleu, J. Maddaluno, I. Chataigner, M. Penhoat, F. X. Felpin, P. Giraudeau and J. Legros, *Angew. Chem., Int. Ed.*, 2017, **56**, 7568–7572.
21 A. Delaune, S. Mansour, B. Picard, P. Carrasqueira, I. Chataigner, L. Jean, P. Y. Renard, J.-C. M. Monbaliu and J. Legros, *Green Chem.*, 2021, **23**, 2925–2930.
22 V. E. H. Kassin, D. V. Silva-Brenes, T. Bernard, J. Legros and J.-C. M. Monbaliu, *Green Chem.*, 2022, **24**, 3167–3179.
23 J. Lavoie, S. Srinivasan and R. Nagarajan, *J. Hazard. Mater.*, 2011, **194**, 85–91.
24 K. Wojciechowskl, *Org. Prep. Proced. Int.*, 1988, **20**, 493–496.
25 Y. Yuan, X. Shi and W. Liu, *Synlett*, 2011, 559–564.
26 M. J. Frisch, G. W. Trucks, H. B. Schlegel, G. E. Scuseria, M. A. Robb, J. R. Cheeseman, G. Scalmani, V. Barone, G. A. Petersson, H. Nakatsuji, X. Li, M. Caricato, A. V. Marenich, J. Bloino, B. G. Janesko, R. Gomperts, B. Mennucci, H. P. Hratchian, J. V. Ortiz, A. F. Izmaylov, J. L. Sonnenberg, D. Williams-Young, F. Ding, F. Lipparini, F. Egidi, J. Goings, B. Peng, A. Petrone, T. Henderson, D. Ranasinghe, V. G. Zakrzewski, J. Gao, N. Rega, G. Zheng, W. Liang, M. Hada, M. Ehara, K. Toyota, R. Fukuda, J. Hasegawa, M. Ishida, T. Nakajima, Y. Honda, O. Kitao, H. Nakai, T. Vreven, K. Throssell, J. A. Montgomery Jr., J. E. Peralta, F. Ogliaro, M. J. Bearpark, J. J. Heyd, E. N. Brothers, K. N. Kudin, V. N. Staroverov, T. A. Keith, R. Kobayashi, J. Normand, K. Raghavachari, A. P. Rendell, J. C. Burant, S. S. Iyengar, J. Tomasi, M. Cossi, J. M. Millam, M. Klene, C. Adamo, R. Cammi, J. W. Ochterski, R. L. Martin, K. Morokuma, O. Farkas, J. B. Foresman and D. J. Fox, *Gaussian 16, Revision C.01*, Gaussian, Inc., Wallingford CT, 2019.
27 I. Funes-Ardoiz and R. S. Paton, *GoodVibes (v3.0.0)*, Zenodo, 2019, DOI: **10.5281/zenodo.33461662018**.
28 J.-C. M. Monbaliu and P. Bianchi, *SnapPy (v1.0.0)*, Zenodo, 2023, DOI: **10.5281/zenodo.8116089**.
29 L. R. Domingo, M. Ríos-Gutiérrez and P. Pérez, *Molecules*, 2016, **21**, 748.
30 P. Geerlings, F. De Proft and W. Langenaeker, *Chem. Rev.*, 2003, **103**, 1793–1873.
31 T. Klöffel, D. Gordon, S. Popiel, J. Nawala, B. Meyer and P. Rodziewicz, *Process Saf. Environ. Prot.*, 2023, **172**, 105–112.
32 Q. E. Thompson, *J. Am. Chem. Soc.*, 1961, **845**, 845–851.
33 K. D. Nagy, B. Shen, T. F. Jamison and K. F. Jensen, *Org. Process Res. Dev.*, 2012, **16**, 976–981.
34 L. Wan, M. Jiang, D. Cheng, M. Liu and F. Chen, *React. Chem. Eng.*, 2022, **7**, 490–550.
35 M. Vaz, D. Courboin, M. Winter and P. M. C. Roth, *Org. Process Res. Dev.*, 2021, **25**, 1589–1597.
36 D. Polterauer, D. M. Roberge, P. Hanselmann, P. Elsner, C. A. Hone and C. O. Kappe, *React. Chem. Eng.*, 2021, **6**, 2253–2258.
37 F. Lou, Q. Cao, C. Zhang, N. Ai, Q. Wang and J. Zhang, *J. Flow Chem.*, 2022, **12**, 307–315.
38 K. Lee, H. Lin and K. F. Jensen, *React. Chem. Eng.*, 2017, **2**, 696–702.

39 M. Irfan, T. N. Glasnov and C. O. Kappe, *Org. Lett.*, 2011, **13**, 984–987.
40 M. J. Nieves-Remacha and K. F. Jensen, *J. Flow Chem.*, 2015, **5**, 160–165.
41 M. O'Brien, I. R. Baxendale and S. V. Ley, *Org. Lett.*, 2010, **12**, 1596–1598.
42 Q. Q. Wang, R. A. Begum, V. W. Day and K. Bowman-James, *Org. Biomol. Chem.*, 2012, **10**, 8786–8793.
43 F. Aricò, M. Chiurato, J. Peltier and P. Tundo, *Eur. J. Org. Chem.*, 2012, 3223–3228.
44 F. Aricò, S. Evaristo and P. Tundo, *ACS Sustainable Chem. Eng.*, 2013, **1**, 1319–1325.
45 D. V. Silva-Brenes, N. Emmanuel, V. López Mejías, J. Duconge, C. Vlaar, T. Stelzer and J.-C. M. Monbaliu, *Green Chem.*, 2022, **24**, 2094–2103.
46 V. E. H. Kassin, R. Morodo, T. Toupy, I. Jacquemin, K. Van Hecke, R. Robiette and J.-C. M. Monbaliu, *Green Chem.*, 2021, **23**, 2336–2351.
47 R. Morodo, R. Gérardy, G. Petit and J.-C. M. Monbaliu, *Green Chem.*, 2019, **21**, 4422–4433.
48 N. Emmanuel, C. Mendoza, M. Winter, C. R. Horn, A. Vizza, L. Dreesen and J.-C. M. Monbaliu, *Org. Process Res. Dev.*, 2017, **21**, 1435–1438.